Journal of Magnetic Resonance **157,** 43–51 (2002)
doi:10.1006/jmre.2002.2573

Proton Dipolar Recoupling in Resin-Bound Peptides under High-Resolution Magic Angle Spinning

Jésus Raya,* Alberto Bianco,† Julien Furrer,* Jean-Paul Briand,† Martial Piotto,‡ and Karim Elbayed*

*Institut de Chimie, UMR 7510 CNRS-Bruker, Université Louis Pasteur, Strasbourg, France; †Institut de Biologie Moléculaire et Cellulaire, Immunologie et Chimie Thérapeutiques, UPR 9021 CNRS, Strasbourg, France; and ‡UMR 7510 CNRS-Bruker, 34 rue de l'industrie, 67166 Wissembourg, France

Received December 13, 2001

Rotational resonance and radiofrequency-driven dipolar recoupling (RFDR) experiments have been used to recover the weak proton dipolar interaction present in peptides bound to swollen resins spun at the magic angle. The intensity of the correlation peaks obtained using these sequences is shown to be significantly stronger than the one obtained using the classical NOESY experiment. In addition, it is found that during the relatively long mixing times required to transfer magnetization in such soft materials, the RFDR sequence also achieves magnetization transfer via the scalar *J*-coupling. © 2002 Elsevier Science (USA)

Key Words: **HRMAS; dipolar recoupling; rotational resonance; radiofrequency-driven dipolar recoupling; NOE; peptides.**

INTRODUCTION

High resolution magic angle spinning (HRMAS) (*1, 2*) is a powerful tool for the characterization of molecules bound to swollen resins (*3–14*), swollen polymers (*15*), or other soft materials such as lipid membranes (*16, 17*), biological tissues (*18, 19*), or fluids contained in solid media (*20*). The linewidth observed in the static ^{1}H NMR spectra of such samples originates mainly from large variations in the bulk magnetic susceptibility of the sample (*14, 21*). Spinning the sample at the magic angle allows for averaging out to zero the effect of the magnetic susceptibility gradients and for achieving a considerable decrease in the NMR linewidth. Magic angle spinning (MAS) also averages out residual anisotropic interactions like the homonuclear proton dipolar coupling and the chemical shift anisotropy (CSA). Due to the fast dynamics of such systems, the dipolar and the CSA interaction are much weaker than those of real solid samples and previous studies have shown that the line broadening due to these interactions is inferior to about 300 Hz (*11, 21*). Liquid state NMR techniques are therefore applicable to such samples under MAS conditions and are routinely employed in the analysis and characterization of compounds attached to solid supports (*11, 13*). In particular, two-dimensional experiments based on coherent transfer of magnetization through the scalar *J*-coupling (TOCSY (*22, 23*) and DIPSI-2 (*24, 25*)) and on incoherent transfer of magnetization through proton–proton cross relaxation effects (NOESY (*26*) and ROESY (*27*)) are particularly powerful.

In a real solid, the measurement of the dipolar coupling between two spins is a convenient technique to determine spatial connectivities and internuclear distances. The intensity of the dipolar coupling follows a $1/r^3$ dependence that makes it a very useful tool for such studies (*28–30*). Compared to the $1/r^6$ dependence of the NOE effect which is used in liquid state NMR, the direct measurement of the dipolar coupling in solids allows, in principle, the determination of longer distances. Unfortunately, under fast magic angle spinning, the dipolar interaction is averaged out to zero and the dipolar coupling is no longer directly measurable. Techniques to recouple the dipolar interaction under MAS are therefore necessary and this field of research has been particularly active for the past 10 years (*31–40*). Most MAS dipolar recoupling experiments use a mixing time during which the dipolar interaction is reintroduced which leads to a transfer of longitudinal or transversal magnetization between neighboring spins.

As mentioned previously, in a molecule bound to a swollen resin, the homonuclear proton dipolar couplings are greatly reduced by the natural mobility of the sample and are completely removed by the rapid rotation of the sample at the magic angle. It would certainly be of interest to recover these interactions in order to study the potential applications of such information to distance measurements. In principle, the dipolar recoupling experiments already developed for solid state NMR should also be applicable to softer materials. Whereas homonuclear carbon dipolar recoupling experiments are used in solid state NMR, it would be of interest, for HRMAS samples, to recover instead the homonuclear proton dipolar coupling in order to have access to proton–proton connectivities.

In this paper, we show that proton dipolar recoupling under MAS can be achieved on compounds bound to swollen resins using rotational resonance (RR) (*31–34*) and radiofrequency-driven dipolar recoupling (RFDR) (*39–42*) techniques. These experiments allow the transfer of longitudinal proton magnetization between dipolar coupled spins and provide information similar to the NOESY experiment (*43*). The RFDR experiment not only recouples the proton dipolar interaction but also allows for transfering magnetization through the scalar *J*-coupling. The results obtained using the RFDR sequence are compared to

1090-7807/02 $35.00

those obtained using the TOBSY (*38, 44*) and DIPSI-2 (*24, 25*) experiments.

RESULTS AND DISCUSSION

Selective and Broadband Dipolar Recoupling

The sample used to study the effect of recoupling experiments is the tetrapeptide Ala-Ile-Gly-Met covalently linked to a Wang resin via the methionine residue and swollen in DMF-d_7 (*14, 21*). The Wang resin is a cross-linked polystyrene-based resin which is commonly used for solid phase peptide and organic synthesis (*45*). The proton chemical shift assignment of the resin-bound peptide swollen in DMF-d_7 and free in solution of DMSO-d_6 is reported in Table 1.

As a first experiment, the two-dimensional MAS NOESY spectrum of the tetrapeptide bound to the swollen Wang resin was recorded at two different speeds. The mixing time was set to 100 ms and the spinning rate was chosen to be 3.739 kHz (Fig. 1A) and 5 kHz (Fig. 1B). The value of 3.739 kHz corresponds exactly to the frequency difference between the γCH_3 protons of Ile and the NH proton of Gly at 500 MHz and, therefore, fulfills the rotational resonance condition that requires the frequency difference to be a multiple of the spinning rate (*31–34*). Figure 1 shows that both spectra exhibit similar intense cross peaks between the different protons of the Wang resin. This result is expected since cross relaxation processes are particularly efficient in such slow dynamics systems. The spectra also reveal that, at a speed of 3.739 kHz, an intense new correlation peak appears between γCH_3 Ile and NH Gly (Fig. 1A). In the spectrum recorded at 5 kHz this signal is absent, even at the lowest contour levels. The presence of this intense cross peak spinning at 3.739 kHz must therefore be due to the recoupling effect of the weak dipolar interaction between NH Gly and γCH_3 Ile.

Whereas rotational resonance produces a highly selective recoupling between neighboring dipolar coupled spins, RFDR permits achieving broadband dipolar recoupling (*39, 41, 42*) using a train of rotor-synchronized proton π pulses. This method was implemented into the mixing time of a standard two-dimensional NOESY sequence. During the mixing time, broadband dipolar recoupling is achieved and magnetization transfer occurs throughout the proton network. It is important to observe that transfers through relaxation effects (NOE) will also take place during the mixing time and it is therefore essential to compare the results obtained using the RFDR experiment with those obtained using a standard NOESY sequence. Figure 1C shows the 2D MAS RFDR spectra of the bound tetrapeptide sample acquired again with a mixing time of 100 ms and at a spinning rate of 5 kHz. Figure 1B shows the result of the NOESY experiment recorded exactly under the same conditions. The difference between both spectra is dramatic. A whole series of new cross peaks between peptide protons can be observed in the RFDR spectrum. This result suggests that the new correlation peaks must be due to a transfer of magnetization between dipolar coupled spins and that broadband proton dipolar recoupling has indeed occurred. The Wang resin, which is much less mobile than the bound peptide and should therefore exhibit larger residual dipolar couplings, also shows a substantial enhancement of its cross peaks.

The effect of the J-coupling during the RFDR sequence applied on such soft materials should however be considered in greater detail. Indeed, the application of high-power π pulses every 200 μs (1/5000 Hz) during the mixing time makes this experiment very similar to the DIPSI-2 experiments (*46*) that use composite π pulses to achieve isotropic mixing throughout the J-coupled network. This point will be further discussed later.

In order to analyze the data of the rotational resonance and of the RFDR experiment, it is therefore important to focus on cross peaks between protons that have no scalar couplings. The cross peak between γCH_3 Ile and NH Gly fulfills this condition and it is used to study the effect of the different recoupling sequences. Figure 2 displays the evolution of the intensities of the diagonal NH Gly and of the NH Gly–γCH_3 Ile cross peak as a function of the mixing time using NOESY, RR, and RFDR experiments. The curves were normalized with respect to the intensity of the diagonal NH Gly obtained at zero mixing time. During the mixing time, correlation peaks result from longitudinal magnetization transfer between dipolar coupled spins. The magnetization transfer can be induced either by dipolar relaxation (NOE) or by transfer through the recoupled dipolar couplings (no J-transfer is possible for this specific spin network). The difference in the cross-peak behavior between the NOESY and the RR experiment is dramatic. Within 150 ms, the RR cross peak reaches an intensity equal to 23.5% of the diagonal. This level of magnetization transfer cannot be achieved

TABLE 1

Proton Chemical Shift Assignment of the Tetrapeptide Ala-Ile-Gly-Met Bound to a Wang Resin Swollen in DMF-d_7 and Free in Solution of DMSO-d_6

	δ (^{1}H) (ppm)	
	Bound	Free
CH_3 Met	2.06	2.13
γCH_3 Ile	1.01	0.98
δCH_3 Ile	0.93	0.89
CH_3 Ala	1.31	1.60
γCH_2 Met	2.59	2.60
βCH_2 Met	2.12	2.13/2.02
γCH_2 Ile	1.65/1.25	1.60/1.23
βCH Ile	1.97	1.92
αCH Met	4.67	4.58
αCH Ile	4.33	4.39
αCH_2 Gly	4.00	3.97
αCH Ala	3.53	4.36
NH Met	8.25	8.08
NH Ile	8.14	8.67
NH Gly	8.48	8.34
Resin aromatic region	7.45–6.40	—
Resin aliphatic region	2.16–1.10	—

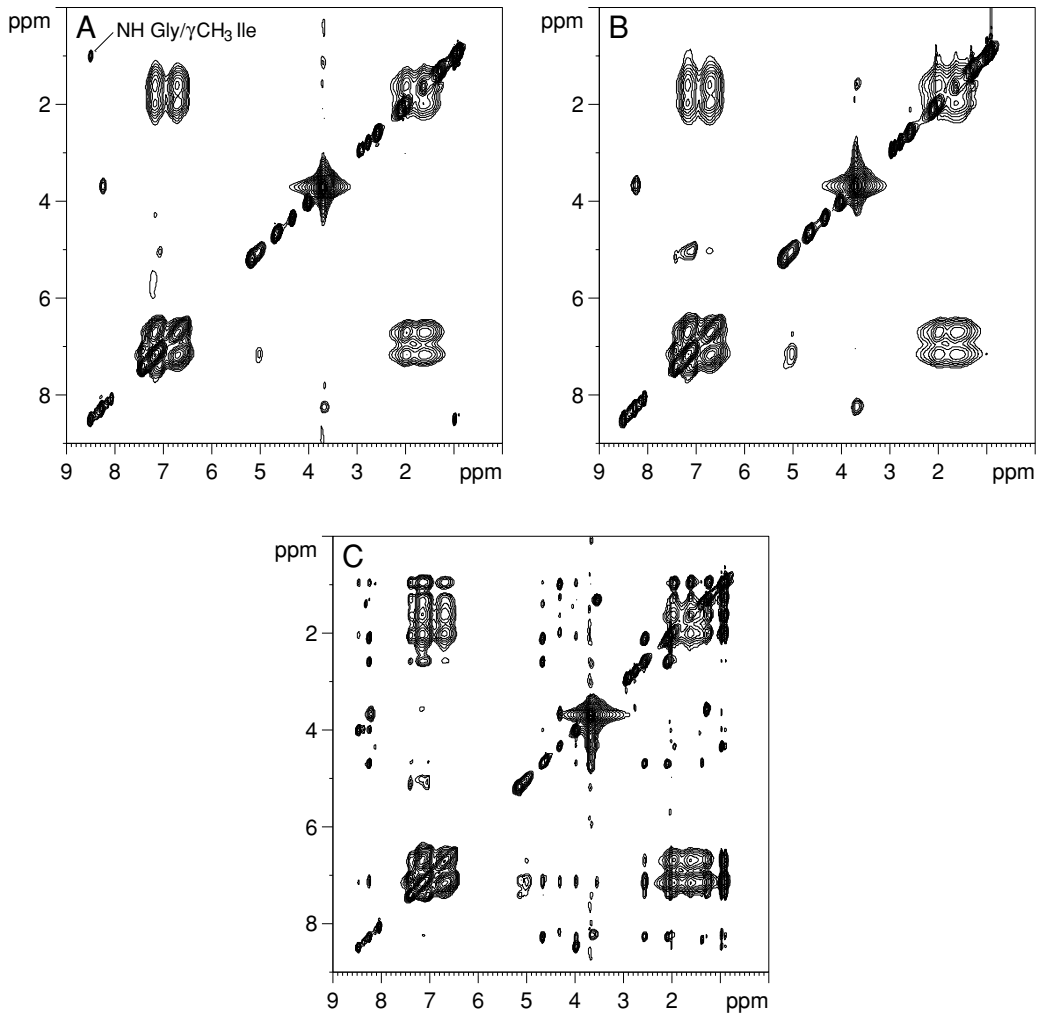

FIG. 1. The 500-MHz ^{1}H 2D MAS rotor-synchronized NOESY/RR (A), NOESY (B), and RFDR (C) spectra of the tetrapeptide Ala-Ile-Gly-Met bound to a Wang resin via the methionine residue and swollen in DMF-d_7. These spectra were acquired with two values for the spinning rate, 3.739 kHz (A) and 5 kHz (B and C), a mixing time of 100 ms, and a B_1 field strength of 55 kHz for the pulses. For the rotor-synchronized NOESY/RR (A) spectrum, the spinning rate was set equal to the frequency difference between the NH Gly and the γCH$_3$ Ile. For the RFDR experiment (C), π pulses were applied every rotor period (i.e., every 200 μs for a speed of 5 kHz). Spectra were recorded on a Bruker DSX-500 spectrometer equipped with a ^{1}H/X MAS probe. Samples were packed into a 50 μl HRMAS rotor and solvent was added directly inside the rotor. Acquisition and processing parameters were sweep width 12 ppm, recycle delay 5 s, 8 scans, 256 $\times$ 1024 complex points, squared sine bell apodization with $\pi/2$ shift in both dimensions. States-TPPI detection was used for the NOESY experiments (A and B) and TPPI detection for RFDR (C).

with the NOE effect. Moreover, this cross peak never appears in the NOESY spectra, even at a mixing time of 500 ms. In the meantime, the diagonal peak of the RR experiment decays to 40% of its value because part of the magnetization is transferred to the cross peak. Compared to the RR experiment, the RFDR experiment exhibits less intense diagonal and correlation peaks. The observed attenuation in the intensity may be ascribed partly to the loss of magnetization due to the numerous π pulses and mainly to the distribution of the dipolar interaction. This behavior is expected since the RFDR technique induces broad band dipolar recoupling and the total magnetization is shared between all the protons in the vicinity of NH Gly and γCH$_3$ Ile. This is also visible in the RFDR diagonal peak intensity which decays much faster than the one of NOESY and RR experiments.

The intensities of NOESY and RFDR peaks as a function of the mixing time were analyzed for a series of proton pairs of the tetrapeptide. In all cases, RFDR and NOE build-up curves present features similar to that described above (data not shown). The RFDR enhancement is more pronounced for proton systems where the NOE contribution is more important. This result is not surprising since both interactions are dipolar and therefore distance dependant. In addition to the difference in cross-peak intensities, the NOE acts at mixing times (300–400 ms) larger than those required for RFDR experiments (50–150 ms).

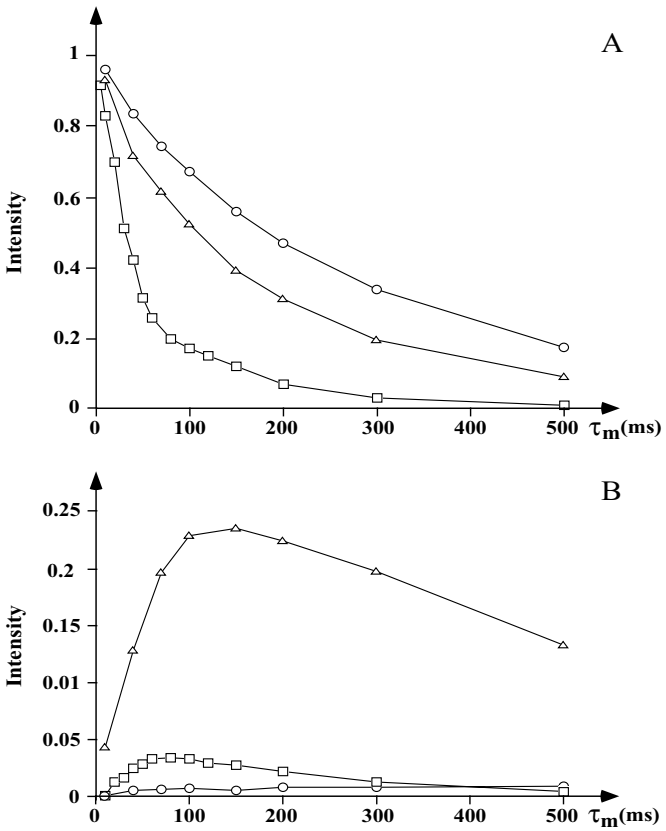

FIG. 2. Intensities of the diagonal NH Gly (A) and of the NH Gly–γCH_3 Ile (B) cross peak as a function of the mixing time using NOESY, RR, and RFDR experiments. Experimental and processing parameters are indicated in Fig. 1. Open circles, triangles, and squares represent the intensities obtained with NOESY, RR, and RFDR experiments, respectively. The curves were normalized with respect to the diagonal peak intensity of NH Gly recorded at zero mixing time.

Compared to a rigid solid, the dipolar recoupling process is quite different in a swollen sample. In the former case, the dipolar coupling between two isolated spins is potentially strong due to the $1/r^3$ distance dependence of the dipolar interaction and the magnetization transfer is a coherent process. In the swollen resin-bound tetrapeptide, the fast dynamics of the system greatly reduces the dipolar coupling since low spinning rates ($<$300 Hz) are sufficient to average it out (*14, 21*). The weak intensity of these interactions explains the long mixing times (50–150 ms) required by the RR and RFDR experiments. This situation bears some similarities to the one described experimentally and theoretically on solid state compounds (*31–33, 39, 47–51*). In the case of weak dipolar couplings and of a network of dipolar coupled spins, the intensity of the dipolar coupling between two spins does not follow a $1/r^3$ distance dependence anymore but follows a $1/r^6$ law which gives rise to a magnetization transfer process which is incoherent. It is important to underline that, under such conditions, the spectral densities are no longer the same as the ones that govern the NOE effect and the new spectral densities lead to cross relaxation rates that are larger than those of NOE (*31, 33, 47, 51*). This difference in the relaxation rates explains the difference in the intensity of the cross peaks observed between the RR, RFDR, and NOESY experiments. By analogy with the relaxation process which is incoherent, the dipolar recoupling by RR and RFDR has been called rotor-driven and RF-driven spin-diffusion (*33, 51*). The determination of the residual proton dipolar coupling is of great interest to obtain dynamics and distance information. In the case of the swollen tetrapeptide sample, the complexity of the proton dipolar coupling network makes a quantitative analysis of the RR and RFDR data quite difficult. However, these results are still very important from a qualitative point of view since they allow for proving the spatial proximity of two protons. Depending on the distance and the mixing time used, this information might not be detectable in a standard NOESY experiment.

Transfer through *J*-Coupling During RFDR Mixing

As mentioned previously, the analysis of the RFDR experiment is further complicated in the case of J-coupled spins by transfers through the J-coupling induced by the π pulses of the RFDR experiment. As a first experimental proof, a RFDR pulse sequence using exactly the same conditions as those of Fig. 1C was performed at 6 kHz instead of 5 kHz. Under these conditions, the π pulses are no longer rotation-synchronized and the outcome of the experiment is significantly different (Fig. 3A). Over 30 cross peaks are absent from the spectrum recorded at 6 kHz. All these missing cross peaks correspond to correlations between resonances that are dipolar coupled but not J-coupled. At 6 kHz, the pulses of the RFDR are no longer rotor-synchronized and the dipolar recoupling becomes certainly less efficient. It must be mentioned that, at 5 kHz, a variation of $\pm$40 Hz in the spinning speed causes the cancellation of the cross peaks arising from dipolar-coupled peptide resonances whereas a variation of $\pm$500 Hz cancels the cross peaks arising from the resin protons. Regarding the cross peaks present in both RFDR spectra recorded at 5 and 6 kHz, a careful examination allows for concluding that they all correspond to J-scalar coupled protons. In fact, all the correlations that are expected from a given J-coupled spin system are present. To proceed further with the analysis of the transfer through J-coupling that occurs during RFDR experiments, the TOBSY (*38, 44*) and DIPSI-2 (*24, 25*) were recorded on the same sample. These experiments were specifically designed to achieve coherence transfer using the J-coupling in solids (TOBSY) and in liquids (DIPSI-2). The results obtained (Figs. 3B and 3C) show that, for the tetrapeptide, both experiments lead to the same series of cross peaks as the RFDR experiment of Fig. 3A. The absence of resin peaks in the DIPSI-2 and TOBSY spectra is not surprising since the protons of the resin have short T_2 and $T_{1\rho}$ values and the long mixing time used in these experiments greatly attenuates the intensity of their signals.

To confirm these results, 2D RFDR and DIPSI-2 experiments were performed on the tetrapeptide Ala-Ile-Gly-Met free in

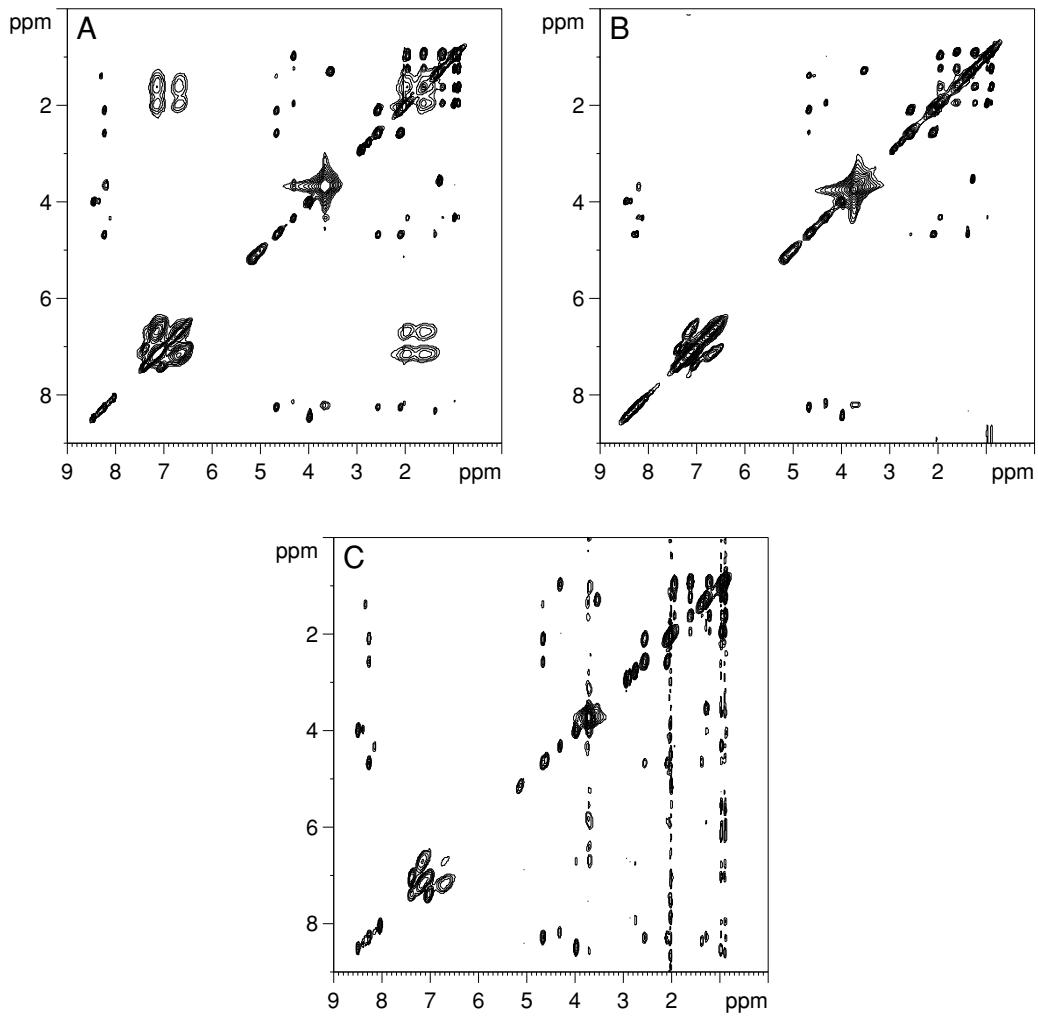

FIG. 3. The 500-MHz ^{1}H 2D MAS "nonsynchronized" RFDR (A), TOBSY (B), and DIPSI-2 (C) spectra of the tetrapeptide-Wang sample swollen in DMF-d_7. These spectra were acquired at spinning rates of 6 kHz (A), 4.166 kHz (B), and 5 kHz (C), with the mixing times, 100 ms (A), 20 ms (B), and 48.7 ms (C), and using the B_1 field strengths, 55 kHz (A, C) and 50 kHz (B). For the "nonsynchronized" RFDR (A), the π pulses period of 5 kHz differs from the MAS rotor period which is 6 kHz. For TOBSY (B), the spinning rate (4.166 kHz) and the B_1 field strength (50 kHz) were chosen in such a manner that the composite RF sequence ($\overline{180}$ 360 $\overline{180}$ 270 $\overline{90}$) is repeated 4 times per rotor period. The longitudinal component of the magnetization was used for the transfer during the TOBSY mixing. For DIPSI-2 (C), the B_1 field strengths were 55 kHz for the high-power $\pi/2$ pulses and 5 kHz for the mixing pulses. For all spectra, acquisition and processing parameters were spectral width, 12 ppm; recycle delay, 3 s; 8 scans; 256×1024 complex points; squared sine bell apodization with $\pi/2$ shift in both dimensions. States-TPPI detection was used for TOBSY (B) and TPPI detection for RFDR (A) and DIPSI-2 (C). The other experimental conditions were the same as for Fig. 1.

solution. This sample behaves fully isotropically and should consequently not exhibit any dipolar interaction. The rapid dynamics of this system is also responsible for an extremely weak NOE effect (data not shown). The proton chemical shift assignment of the peptide free in solution of DMSO-d_6 is reported in Table 1. The 2D RFDR and DIPSI-2 spectra shown in Figs. 4A and 4B were acquired with the same experimental conditions as those of Fig. 1C. For both experiments, the same mixing time (80 ms) was used. The spectra display similar cross peaks that all correspond to J-scalar coupled protons. Experiments recorded using a liquid probe on the same tetrapeptide free in solution also show that the RFDR sequence leads to a spectrum characterized by cross peaks originating from J-coupled protons. These results thus obtained prove that the J-coupling can give rise to correlation peaks in RFDR experiments.

These experimental observations can as well be proven theoretically. Calculations of the transfer of magnetization through the J-coupling of the longitudinal component were performed in the case of a J-scalar coupled IS spin pair (spins 1/2). The magnetization transfer can be tracked by calculating the difference in Zeeman magnetization $\langle I_z - S_z \rangle$ obtained after a selective inversion. The evolution of the density matrix was calculated by numerical integration of the equation of motion according to (*28*)

$$\rho(t + \Delta t) = \exp(-iH(t)\Delta t)\rho(t)\ \exp(iH(t)\Delta t),$$

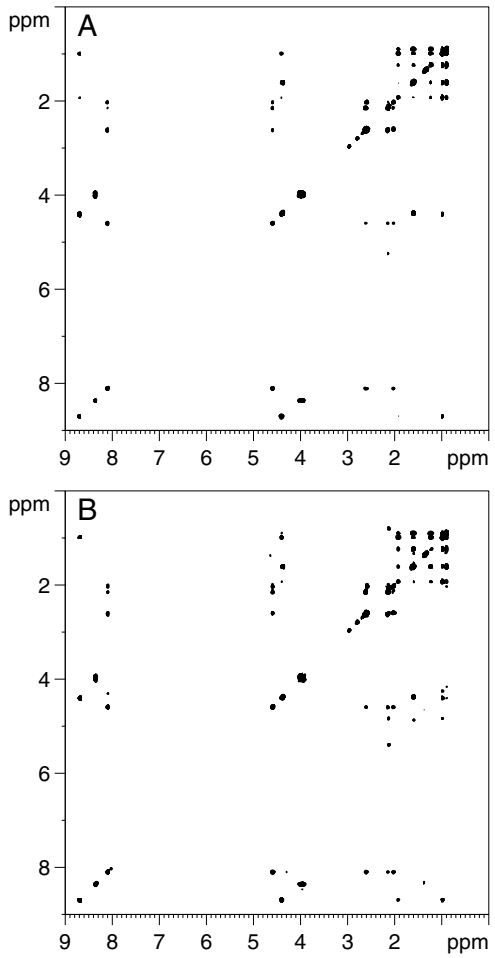

FIG. 4. The 500-MHz ^{1}H 2D RFDR (A) and DIPSI-2 (B) spectra recorded on the tetrapeptide Ala-Ile-Gly-Met free in solution of DMSO-d_6. Spectra have been acquired with the same conditions as those reported in Fig. 3. Both spectra were acquired at a spinning rate of 5 kHz, with a mixing time of 80 ms and a B_1 field strength of 45 kHz. For the DIPSI-2 mixing pulses a field strength of 5 kHz was used. Acquisition and processing parameters were spectral width, 12 ppm; recycle delay, 5 s; 8 scans; 256 × 1024 complex points; squared sine bell apodization with $\pi/2$ shift in both dimensions. TPPI detection was used for both experiments.

where $\rho(t)$ is the density matrix representing the state of the system and $H(t)$ is the time-dependent Hamiltonian. $H(t)$ is given by

$$H(t) = \Omega_I I_z + (\Omega_I + \Delta\Omega_{IS})S_z + J_{IS} IS + H_{RF}(t),$$

where Ω_I is the chemical shift of spin I, Ω_{IS} is the difference in chemical shift between I and S, J_{IS} is the J-coupling set to 10 Hz, and $H_{RF}(t)$ is the π-pulse train used in the RFDR sequence. Simulations were carried out using the conditions of the RFDR experiment with π-pulses of 55 kHz spaced by a delay of 200 μs. The numerical simulations show a sinusoidal behavior of the $\langle I_z - S_z \rangle$ magnetization. The values of $\Delta\Omega_{IS}$ used (*between* 0 *and* 5000 Hz) correspond to the difference in chemical shift present in our experiment at 500 MHz. For this range of values, the oscillation frequency is found to be about J_{IS}. For larger values of $\Delta\Omega_{IS}$ (>10 ppm), the periodicity of the evolution deviates from J_{IS}. The offset Ω_{IS}, the intensity of the RF field, and the delay between the π-pulses certainly influence the outcome of the simulations; however, the analysis of their effects on the efficiency of the J-transfer is out of the scope of this work. The calculations simply shows that the π pulses used in the 2D RFDR are able to generate magnetization transfer through the J-coupling.

This result is not surprising if the RFDR sequence is compared to the DIPSI-2rc (*46*) experiment. This sequence uses composite π pulses separated by a delay period that is adjusted to compensate NOE and ROE effects in order to obtain pure J-correlation spectra. It must be noted that the mixing times used in the RFDR experiments on the bound tetrapeptide are in the same range of values as the ones used for the DIPSI-2rc experiments in liquid state NMR. In the swollen sample, the situation is quite different from a rigid solid where the J-coupling is not taken into account since the dipolar couplings are much stronger and only short mixing times are necessary in RFDR experiments.

It is clear that the existence of several pathways during the transfer of longitudinal magnetization can lead to some ambiguity in the interpretation of proton 2D-RFDR spectra. This can result in an enhancement in the correlations involving J-coupled protons since both coherence transfers have the same sign. The RFDR sequence provides therefore reliable information only in the case of non-J-coupled protons. As mentioned previously, this information is very important since it may not be present in a classical NOESY or ROESY experiment.

Application of RF-Driven Dipolar Recoupling (RFDR)

As a second example of the application of the RFDR experiment to real systems, the retro-inverso (RI) analogue (*52*) of the 141–159 peptide corresponding to the VP1 region of Foot-and-Mouth Disease Virus (FMDV) (*53*) bound to polystyrene-based MBHA (methylbenzhydrylamine) resin through the C-terminal Gly residue was subjected to dipolar recoupling experiments. The sequence of the RI-FMDV peptide ^{141}LQRAVRPALSGFDGRVGSG^{159} was built on the resin using D-amino acids and classical solid phase chemistry. An additional 6-aminohexanoic acid residue (Ahx) was added to the C-terminal part of the peptide in order to have a spacer between the peptide and the resin, while the N-terminal part of the peptide was acetylated. The identification of the amino acid spin system and the sequential assignment were made using a combination of HRMAS DIPSI-2, NOESY, and HSQC experiments (*54*). The 2D spectra of this resin-bound oligomer contain several hundred resonances and the detection of new cross peaks arising from residual dipolar coupling can be difficult. A series of RFDR, NOESY, and DIPSI-2 experiments were recorded at 20, 50, and 80 ms mixing time. The mixing times were chosen on the basis of the previous results obtained with the tetrapeptide for which the

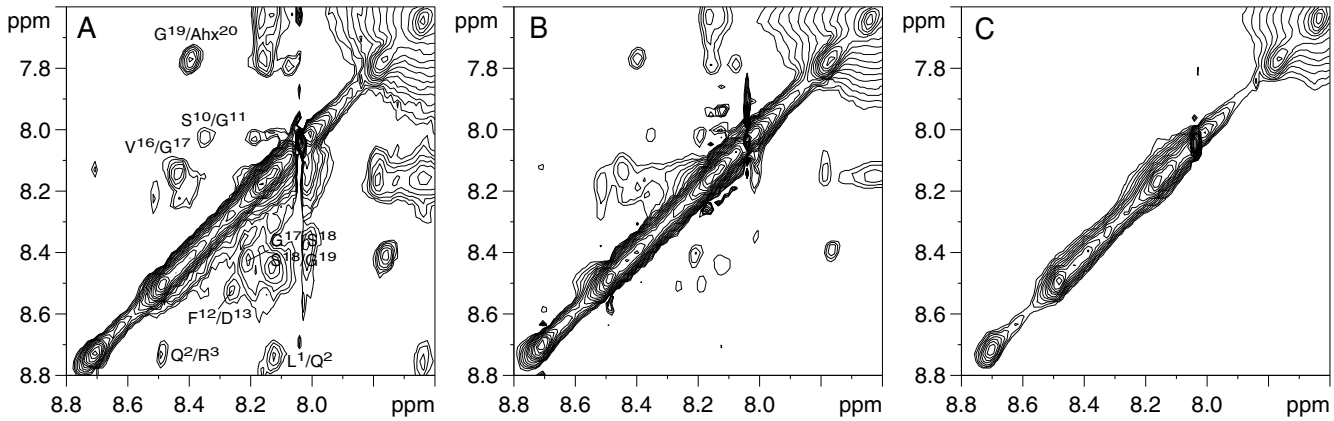

FIG. 5. The 500-MHz NH–NH region of the MAS RFDR (A), NOESY (B), and DIPSI-2 (C) spectra ($\tau_m = 80$ ms) recorded on the RI-FMDV peptide bound to MBHA resin swollen in DMF-d_7. The residues are numbered from Leu 1 to Ahx 20. Spectra were recorded on a DRX-500 Bruker spectrometers equipped with ^{1}H/^{2}D/^{13}C HRMAS probes, respectively. The HRMAS probe was equipped with a magic angle gradient. Spectra were acquired at a spinning rate of 5 kHz and with a B_1 field strength of 35 kHz for the high-power $\pi/2$ pulses. A B_1 field strength of 15.6 kHz was employed for the π pulses of the RFDR mixing pulses (A) and of 8.3 kHz for the DIPSI-2 mixing pulses (B). Acquisition and processing parameters were spectral width, 12 ppm; recycle delay, 3 s; 8 scans; 256 × 1024 complex points; squared sine bell apodization with $\pi/2$ shift in both dimensions. States-TPPI detection was used for both experiments.

cross-peak maximum intensities were found around 80 ms. We initially focus our attention on the analysis of the amide region which does not contain any J-coupling cross peaks. The 80-ms RFDR, NOESY, and DIPSI-2 spectra of the amide–amide region recorded on the RI-FMDV peptide bound to MBHA resin swollen in DMF-d_7 are reported in Fig. 5. The difference between the three spectra is astonishing. While the NOESY spectrum (Fig. 5B) exhibits very weak cross peaks, those present in the RFDR (Fig. 5A) are very intense, showing that residual dipolar recoupling between the amide protons has occurred. These

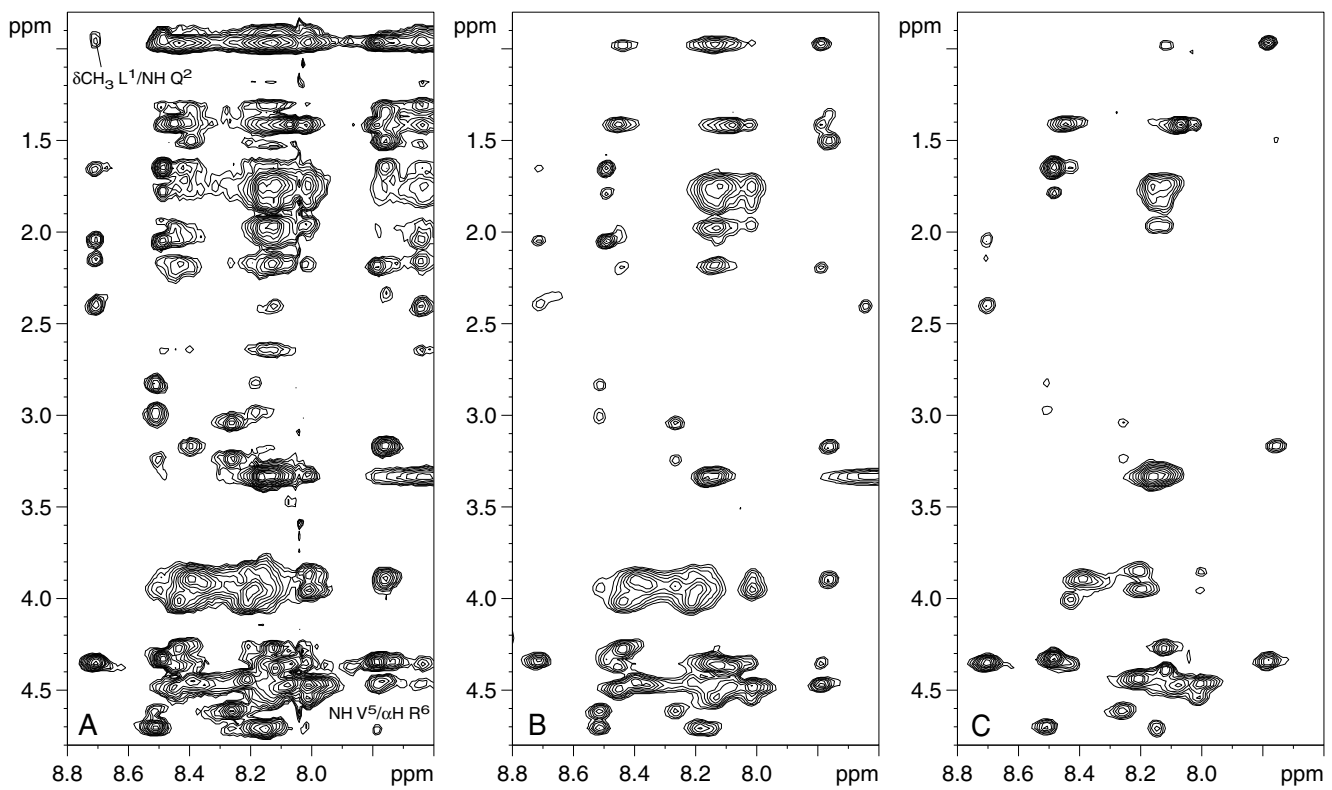

FIG. 6. The 500-MHz fingerprint and amide-side chain region of the MAS RFDR (A), NOESY (B), and DIPSI-2 (C) spectra ($\tau_m = 80$ ms) recorded on the RI-FMDV peptide bound to MBHA resin swollen in DMF-d_7. The residues are numbered from Leu 1 to Ahx 20. The other experimental conditions are the same as those of Fig. 5.

cross peaks are absent from the DIPSI-2 experiment (Fig. 5C). It must be noted, however, that in this region, similar NH–NH correlations could be detected with a NOESY experiment performed using a longer mixing time (300 ms) (data not shown). The difference in intensity of the cross peaks is also evident in the spectra corresponding to the fingerprint and amide-side chain region of the 80-ms RFDR, NOESY, and DIPSI-2 experiments (Fig. 6). Besides their higher intensity, new cross peaks have also appeared between δCH_3 of Leu1 and NH of Gln2 and between NH of Val5 and αH of Arg6, for example. These signals are absent from the NOESY recorded at τ_m of 80 ms, although they begin to appear with a very weak intensity using longer mixing times (*54*). These findings are very promising and demonstrate that RFDR experiments can be successfully applied to long peptides. The additional information which is provided by the RFDR spectra could be useful not only for sequence assignment but also for structural characterization of resin bound molecules. Work in this direction, including determination of the secondary structure of peptides bound to different solid supports by means of RFDR experiments, is in due course.

CONCLUSION

In conclusion, we have shown that for both the tetrapeptide Ala-Ile-Gly-Met and the 141–159 retro-inverso peptide analogue from Foot-and-Mouth disease Virus bound to polystyrene-type resins, the residual proton dipolar coupling is high enough to be observed in dipolar recoupling experiments. The results obtained show that RR and RFDR techniques can be employed for recovering proton dipolar interactions in molecules bound to swollen resin. In a 2D RFDR spectrum, correlations can originate either from dipolar recoupling, cross relaxation, or from J-coupling. In the case of two protons that are not J-coupled, the presence of a correlation peak is extremely important information since it proves the spatial proximity of these two protons. The intensity of this peak, which is much stronger than a regular NOE peak, should allow the detection of longer distances even though the interaction still seems to follow a $1/r^6$ dependence. As shown for the RI-FMDV peptide, correlations between nuclei, that cannot be detected using the classical NOESY experiment, are present in the RFDR spectrum. At this stage, it is difficult to extract quantitative data from these experimental results and to have access to distance information. Clearly, the application of proton dipolar recoupling to the study of soft materials needs to be better studied and more research on this topic in currently under way. In particular the analysis of this phenomenon using simpler proton and carbon spin systems should allow a better understanding of the phenomena involved.

REFERENCES

1. E. R. Andrew, A. Bradbury, and R. G. Eades, *Nature* **182,** 1659 (1958).
2. I. J. Lowe, *Phys. Rev. Lett.* **2,** 285 (1959).
3. W. L. Filtch, G. Detre, C. P. Holmes, J. N. Scoorley, and P. A. Keifer, *J. Org. Chem.* **59,** 7955 (1994).
4. R. C. Anderson, M. A. Jarema, M. J. Shapiro, J. P. Stockes, and M. Zilliox, *J. Org. Chem.* **60,** 2650 (1995).
5. R. C. Anderson, J. P. Stockes, and M. J. Shapiro, *Tetrahedron Lett.* **36,** 5311 (1995).
6. P. A. Keifer, *J. Org. Chem.* **61,** 1558 (1996).
7. I. E. Pop, C. F. Dhalluin, B. P. Déprez, P. C. Melnyk, G. M. Lippens, and A. L. Tartar, *Tetrahedron* **52,** 12209 (1996).
8. C. Dhalluin, C. F. Boutillon, A. Tartar, and G. M. Lippens, *J. Am. Chem. Soc.* **119,** 10494 (1997).
9. R. Jelinek, A. P. Valente, K. G. Valentine, and S. J. Opella, *J. Magn. Reson.* **125,** 185 (1997).
10. M. J. Shapiro, J. Chin, R. E. Marti, and M. A. Jarosinski, *Tetrahedron Lett.* **38,** 1333 (1997).
11. G. M. Lippens, M. Bourdonneau, C. Dhalluin, R. Warrass, T. Richert, C. Seetharaman, C. Boutillon, and M. Piotto, *Curr. Org. Chem.* **3,** 147 (1999).
12. A. Bianco, J. Furrer, D. Limal, G. Guichard, M. Piotto, J. Raya, K. Elbayed, and J. P. Briand, *J. Comb. Chem.* **2,** 681 (2000).
13. J. Furrer, M. Piotto, M. Bourdonneau, G. Guichard, D. Limal, K. Elbayed, J. Raya, J. P. Briand, and A. Bianco, *J. Am. Chem. Soc.* **123,** 4130 (2001).
14. J. Furrer, K. Elbayed, M. Bourdonneau, J. Raya, D. Limal, A. Bianco, and M. Piotto, *Magn. Res. Chem.* **40,** 123 (2002).
15. B. Martel, M. Devassine, G. Crini, M. Weltrowski, M. Bourdonneau, and M. Morcellet, *J. Poly. Sci.* **39,** 169 (2001).
16. J. D. Gross, P. R. Costa, J. B. Dubacq, D. E. Warschawski, P. N. Lirsac, P. F. Devaux, and R. G. Griffin, *J. Magn. Reson. B* **106,** 187 (1995).
17. D. Huster, K. Kuhn, D. Kadereit, H. Waldmann, and K. Arnold, *Angew. Chem. Int. Ed. Engl.* **40,** 1056 (2001).
18. L. L. Chang, C. L. Lean, A. Bogdanova, S. Carter Wright, Jr., J. L. Ackermann, T. J. Brady, and L. Garrido, *Magn. Res. Med.* **36,** 653 (1996).
19. D. Moka, R. Vorreuther, H. Schicha, M. Spraul, E. Humpfer, M. Lipinski, P. J. D. Foxall, J. K. Nicholson, and J. C. Lindon, *Anal. Commun.* **34,** 107 (1997).
20. T. M. de Swiet, M. Tomaselli, M. D. Hürlimann, and A. Pines, *J. Magn. Reson.* **133,** 385 (1998).
21. K. Elbayed, M. Bourdonneau, J. Furrer, T. Richert, J. Raya, J. Hirschinger, and M. Piotto, *J. Magn. Reson.* **136,** 127 (1999).
22. L. Braunschweiler and R. R. Ernst, *J. Magn. Reson.* **53,** 521 (1983).
23. A. Bax and D. G. Davis, *J. Magn. Reson.* **65,** 355 (1985).
24. A. J. Shaka, C. J. Lee, and A. Pines, *J. Magn. Reson.* **77,** 274 (1988).
25. S. P. Rucker and A. J. Shaka, *Mol. Phys.* **68,** 509 (1989).
26. J. Jeener, B. H. Meier, P. Bachmann, and R. R. Ernst, *J. Chem. Phys.* **71,** 4546 (1979).
27. A. A. Bothner-By, R. L. Stephens, J.-M. Lee, C. D. Warren, and R. W. Jeanloz, *J. Am. Chem. Soc.* **106,** 811 (1984).
28. A. Abragam, "The Principles of Nuclear Magnetism," Oxford Univ. Press, London (1961).
29. A. E. Benett, R. G. Griffin, and S. Vega, "NMR Basic Principles and Progress," Vol. 33, Springer-Verlag, Berlin (1994).
30. J. R. Garbow and T. Gullion, "Measurement of Internucleaire Distances in Biological Solids by Magic Angle Spinning 13C NMR, in Carbon-13 NMR Spectroscopy of Biological Systems," Academic Press, New York (1995).
31. E. R. Andrew, A. Bradbury, R. G. Eades, and V. T. Wynn, *Phys. Lett.* **4,** 99 (1963).
32. D. P. Raleigh, M. H. Levitt, and R. G. Griffin, *Chem. Phys. Lett.* **146,** 71 (1988).

33. M. G. Colombo, B. H. Meier, and R. R. Ernst, *Chem. Phys. Lett.* **146,** 189 (1988).

34. M. H. Levitt, D. P. Raleigh, F. Creuzet, and R. G. Griffin, *J. Chem. Phys.* **92,** 6347 (1990).

35. D. M. Gregory, D. J. Mitchell, J. A. Stringer, S. Kiihne, J. C. Shiels, J. Callahan, M. A. Mehta, and G. P. Drobny, *Chem. Phys. Lett.* **246,** 654 (1995).

36. B. Q. Sun, P. R. Costa, D. Kocisko, P. T. Lansburg, and R. G. Griffin, *J. Chem. Phys.* **102,** 702 (1995).

37. Y. K. Lee, N. D. Kurur, M. Helmle, O. Johannessen, N. C. Nielsen, and M. H. Levitt, *Chem. Phys. Lett* **242,** 304 (1995).

38. M. Baldus, R. J. Iuliucci, and B. H. Meier, *J. Am. Chem. Soc.* **119,** 1121 (1997).

39. A. E. Benett, C. M. Rienstra, J. M. Griffiths, W. Zhen, J. Lansbury, P. T. Griffin, and R. G. Griffin, *J. Chem. Phys.* **108,** 9463 (1998).

40. M. Baldus, D. G. Geurts, and B. H. Meier, *Solid State Nucl. Magn. Reson.* **11,** 157 (1998).

41. A. E. Benett, J. H. Ok, R. G. Griffin, and S. Vega, *J. Chem. Phys.* **96,** 8624 (1992).

42. D. K. Sodickson, M. H. Levitt, S. Vega, and R. G. Griffin, *J. Chem. Phys.* **98,** 6742 (1993).

43. J. Furrer, Ph.D. Thesis, Louis Pasteur, Strasbourg, 2001.

44. M. Baldus and B. H. Meier, *J. Magn. Reson. A* **121,** 65 (1996).

45. A. R. Vaino and K. D. Janda, *J. Comb. Chem.* **2,** 579 (2000).

46. J. Cavanagh and M. Rance, *J. Magn. Reson.* **96,** 670 (1992).

47. E. R. Andrew, S. Clough, L. F. Farnell, T. D. Gledhill, and I. Roberts, *Phys. Lett.* **21,** 505 (1966).

48. D. Suter and R. R. Ernst, *Phys. Rev. B* **32,** 5608 (1985).

49. D. L. Vanderhart, *J. Magn. Reson.* **72,** 13 (1987).

50. A. Kubo and C. A. McDowell, *J. Chem. Soc. Faraday Trans. 1* **84,** 3713 (1988).

51. P. Robyr, B. H. Meier, and R. R. Ernst, *Chem. Phys. Lett.* **162,** 417 (1989).

52. M. Chorev and M. Goodman, *Acc. Chem. Res.* **26,** 266 (1993).

53. M.-C. Petit, N. Benkirane, G. Guichard, A. Phan Chan Du, M. Marraud, M. T. Cung, J.-P. Briand, and S. Muller, *J. Biol. Chem.* **274,** 3686 (1999).

54. J. Furrer, M. Piotto, M. Bourdonneau, D. Limal, G. Guichard, K. Elbayed, J. Raya, J. P. Briand, and A. Bianco, manuscript in preparation.